Topical instillation of cell-penetrating peptide-conjugated melphalan blocks metastases of retinoblastoma

Kuan Jiang
Fudan University
Xingyan Fan
Fudan Universiy
Yang Hu
Fudan University
Shengyu Yao
Fudan University
Yu Liu
Fudan University
Changyou Zhan
Fudan University https://orcid.org/0000-0002-5215-2829
Weiyue Lu
Fudan University
Gang Wei (weigang@shmu.edu.cn)
School of Pharmacy, Fudan University https://orcid.org/0000-0002-9600-0982

Article

Keywords: Retinoblastoma, Melphalan, Cell-penetrating peptide, Brain metastases, Eye drops

Posted Date: August 17th, 2021

DOI: https://doi.org/10.21203/rs.3.rs-783746/v1

Version of Record: A version of this preprint was published at Biomaterials on April 1st, 2022. See the published version at https://doi.org/10.1016/j.biomaterials.2022.121493.

Abstract

Retinoblastoma is the most common primary intraocular malignancy in infancy with a metastases-related death risk. However, a safe and convenient treatment without enucleation is still an unmet clinical need. In this work, a cell-penetrating peptide, 89WP, was conjugated with melphalan (89WP-Mel), which achieved comparable tumor inhibition effects to intravitreally injected melphalan via topical instillation for the first time. Notably, the “outside-in” diffusion of instilled 89WP-Mel created a protective shield surrounding the eye, efficiently preventing tumor metastases. In contrast, the mice treated with intravitreally injected melphalan suffered more brain metastases related death, probably due to the “inside-out” diffusion of injected melphalan expelling the tumor outside the eye. The ocular absorption of 89WP-conjugated melphalan and other small molecules, both hydrophobic and hydrophilic, occurred via non-corneal pathway with high safety and a prolonged residence duration in retina up to 24 h. The present work paves a new avenue for simultaneous intraocular tumor inhibition and extraocular metastases prevention in a safe and convenient way via topical instillation.

Introduction

Retinoblastoma (RB) is the most frequent primary intraocular malignancy in infancy and childhood, about 9000 new cases every year[1]. Potential extraocular extension, including brain and bone marrow metastases, causes RB a life-threatening disease[2]. Brain metastases is usually with nearly 100% mortality rate, therefore, preventing metastases is the first priority during treatment of RB[3]. Few years ago, RB was treated only by eye enucleation, leading to a permanent vision loss, but today can be treated by conservative chemotherapy with preservation of functional vision in developed regions[4]. Efficient control of RB requires early detection, following timely and appropriate treatment[5]. Besides, blocking the extraocular spread especially the brain metastases is of vital importance[6].

Interventions such as intra-arterial[7] or intravitreal[8] chemotherapy improve the outcomes in advanced intraocular RB by offering higher doses of drugs in retina and vitreous body. Lack of vasculature structure in the vitreous body makes intravitreal chemotherapy the preferred method for treating sub-retinal and vitreous tumor seeds, and melphalan (20–30 μg/0.1 mL, once a week or on alternate weeks) is the most common used drug[3, 9]. Notably, intravitreal chemotherapy is probably with extraocular tumor extension and metastasis risk via the needle tracks or other routes[6]. Besides, frequent intravitreal injections, mainly due to quick elimination of melphalan in vitreous body[10], request a high-quality medical environment and a practiced clinician, which is scarce in developing regions with limited health care systems[4]. Indeed, a safe and convenient treatment, for example topical instillation, could substantially improve the conditions. Unfortunately, it is difficult for small molecules like melphalan to be delivered into the posterior ocular segment via topical instillation.

Penetratin was previously reported as a more safe and powerful ocular permeation enhancer than several other cell-penetrating peptides[11] and could promote ocular delivery of both small molecules and nucleic

acids[12–16]. By hydrophobic amino acids mutation, various penetratin derivatives were obtained with even better ocular permeability, and tryptophan mutation at the eighth (glutamine) and ninth (asparagine) amino acid residues resulted in an excellent ocular permeable peptide (Q8W, N9W-Penetratin, 89WP)[17]. In this work, covalent conjugate of 89WP and melphalan (89WP-Mel) was constructed to achieve efficient inhibition on intraocular tumor proliferation by topical instillation. It was also postulated that the instilled 89WP-Mel would form a protective shield surrounding the eye through the non-corneal absorption route and siege the intraocular tumor. Besides exploring the mechanisms for 89WP-Mel to hinder brain metastases of RB, the potential of turning melphalan from intravitreal injection to eye drops for RB therapy by conjugation with 89WP was also investigated.

Results

Synthesis and characterization of 89WP conjugates. Harnessing previously designed penetratin derivatives with high permeability to the eye[17], we combined one of powerful derivatives (89WP) with melphalan to explore if topical instillation of the covalent conjugate 89WP-Mel could inhibit intraocular tumor proliferation. Molecular structure, synthetic routes and characterization of conjugates are shown in Fig. 1, S1 and Table 1.

Table 1
Sequence and characterization of 89WP and different conjugates.

Abbreviation	Sequence	Mw (Da)	miLogP*, Mw (Da) of conjugated molecules
89WP	RQIKIWFWWRRMKWKK	2376.95	-
89WP-Mel	RQIKIWFWWRRMKWKK-Mel	2664.15	0.08, 305.20 (Mel)
89WP-FAM	RQIKIWFWWRRMKWKKK-FAM	2863.47	0.56, 504.52 (K-FAM)
Cy5-89WP	Cy5-CRQIKIWFWWRRMKWKK	3245.21	-0.58, 886.26 (Cy5-C)
* Calculated by the Molinspiration Property Calculator tool at https://www.molinspiration.com/cgi-bin/properties.			

Topical instillation of 89WP-Mel inhibited intraocular tumor proliferation and metastases. On an established intraocular tumor-bearing mice model, normal saline (N.S.), melphalan (Mel, 3.0 mg/mL), two different doses of 89WP-Mel (containing 0.3 mg/mL or 3.0 mg/mL melphalan) were topically applied (Topi.) as eye drops (10 μL per eye, once daily). The positive control was set as intravitreal injection of melphalan (IVT. Mel, 8.0 mg/mL, 2 μL per eye, once per month, 16 times more than the regular single dose[18]). After 1-month treatment, the sizes of vitreous seeds in different groups were compared based on

the whole eye sections stained with hematoxylin-eosin. As shown in **Fig. 2A**, the vitreous seeds after the treatment of 89WP-Mel (both low- and high-dose) were much smaller than that in the normal saline treated group. Topical instillation of high-dose 89WP-Mel (89WP-Mel-High) achieved comparable anti-retinoblastoma effects to the positive control (IVT. Mel). However, mice in IVT. Mel treated group suffered unexpected death. Three out of five mice died during the treatment, while only one death occurred in the high-dose 89WP-Mel treated group. According to the immunohistochemical section of the whole brain from a surviving mouse in the group treated by topically instilled melphalan (**Fig. 2B**), an area with distinct GFP signal from the metastasizing retinoblastoma cells emerged in the region of spinal trigeminal nucleus, which connected with the eye via the optic nerve[3].

To verify the anti-metastasis effect of topical instillation of 89WP-Mel, pharmacodynamical evaluation was further implemented with a larger size of samples (n = 8), accompanying with the optimized dose of instilled 89WP-Mel (containing 3.0 mg/mL melphalan, 10 μL/eye, once daily) and adapted dose regimen of intravitreally injected melphalan (0.5 mg/mL, 2 μL/eye, once on alternate weeks). During the 1-month treatment, 89WP-Mel exhibited efficient inhibitory effects against intraocular tumor, which was comparable to intravitreally injected melphalan (Fig. 3B, **Fig. S2**). In contrast, topical instillation of melphalan at the same dose was invalid. The mice treated with 89WP-Mel and intravitreally injected melphalan suffered a much lower intraocular tumor proliferation, registering one-fifth and one-third of the increasing folds of bioluminescence in comparison to the normal saline treated group on the Day 30 ($p < 0.0001$, Fig. 3C). However, there was no statistically significant difference between the groups treated by normal saline and topically instilled melphalan ($p = 0.9087$). More importantly, the mice treated with 89WP-Mel resulted in an improved survival rate, which was even better than those receiving intravitreally injected melphalan (Fig. 3D). Brain metastases were evaluated based on immunohistochemical sections of the brains from moribund mice with a sudden decrease of body weight lower than 21 g (**Fig. S3**), or the surviving mice at the end of the experiment (on the Day 60). Apart from the 89WP-Mel treated group, obvious tumor regions could be found in all the other groups, and the number of mice with positive metastases (namely with proliferative tumor regions) in the brains was respective 3 (Topi. N.S.), 1 (Topi. Mel), and 2 (IVT. Mel) (Fig. 3E, **Fig. S4**, **Fig. S5**). Two survived mice were free of metastatic tumors in the 89WP-Mel treated group, which was evidenced without brown dots distribution in the brain sections.

Covalent conjugation was indispensable for 89WP to promote cellular uptake of small molecules. Static absorption barriers, mainly comprised of corneal epithelial barrier (anterior barrier) and retinal pigment epithelial barrier (posterior barrier), firmly hinder the delivery of topically instilled therapeutics into the posterior ocular segment [19]. Human corneal epithelial cells (HCEC) and human retinal pigment epithelial cells (ARPE-19) were selected to evaluate the cellular uptake of hydrophobic dye 5-carboxyfluorescein (FAM) and hydrophilic dye sulfo-cyanine5 (Cy5) with the aid of 89WP. According to the quantitative results (Fig. 4A, **Fig. S6**), cellular uptake efficiency of the covalent conjugates (89WP-FAM and Cy5-89WP) was approximate 100%, which was much higher than the small molecules alone or their mixtures with 89WP (89WP/FAM and 89WP/Cy5). In HCEC cells, the mean fluorescence intensity of the 89WP-FAM treated cells was respective 37 ($p < 0.001$) and 28 ($p < 0.001$) times higher than the FAM or 89WP/FAM

treated cells. In ARPE-19 cells, the increasing folds were respective 342 ($p < 0.001$) and 272 ($p < 0.001$). For covalent conjugate Cy5-89WP, the increased folds were 125 ($p < 0.001$) and 28 ($p < 0.001$) in HCEC cells, 105 ($p < 0.001$) and 78 ($p < 0.001$) in ARPE-19 cells. Notably, there was no statistically significant difference ($p > 0.05$) in cellular uptake between small molecules and their mixtures with 89WP in two cells, suggesting that covalent conjugation was indispensable to improve cellular uptake of small molecules.

According to intracellular distribution of small molecules and the covalent conjugates in HCEC and ARPE-19 cells (**Fig. S7, S8**), there was no obvious fluorescent signal in FAM or Cy5 treated cells. However, much stronger fluorescence could be observed in the cells treated with the covalent conjugates. More importantly, most of the fluorescence from the covalent conjugates was not co-localized with lysosomes, indicating a potential endosomal escape ability.

To discern cell entry pathways of the covalent conjugates, cellular uptake of 89WP-FAM in ARPE-19 cells was explored in the presence of various inhibitors or at different temperatures[20]. Compared to the uninhibited control group (Fig. 4B), cellular uptake decreased substantially either at low temperature or in the presence of chlorpromazine and hypertonic sucrose, pointing to an energy-dependent and clathrin-mediated endocytosis pathway. The endosomal escape capability of 89WP was evaluated by hemolysis assay. At the concentrations ranging from 40 to 640 μM, hemolysis rate induced by 89WP at pH 5.5 was 2–3 times higher ($p < 0.05$) than that at pH 7.4 (Fig. 4C), further suggesting enhanced endosomal escape of the covalent conjugates.

Sclera was more permeable than cornea for 89WP-conjugated small molecules. The ARPE-19 cell monolayer model was established to evaluate 89WP-FAM permeability across the posterior ocular barriers (**Fig. S9**). As shown in **Fig. S9B**, there was nearly no green fluorescent signal in FAM or 89WP/FAM mixture treated monolayer, but conspicuous fluorescence was observed in the monolayer after the treatment of 89WP-FAM. From the side view (Fig. 5A **(a)**), 89WP-FAM could permeate the whole monolayer. In addition, 89WP-FAM crossed the monolayer in a linearly time-dependent manner within 4 h (Fig. 5A **(b)**). After 4 h incubation, up to 16.5% of the 89WP-FAM was found in the basolateral side, which was 5.5 times more than the free FAM and the 89WP/FAM mixture. Apparent permeability coefficient (P_{app}) of 89WP-FAM was 3.46×10^{-5} cm/s, which was 6 times higher than the others ($p < 0.0001$, Fig. 5A **(c)**). After penetrating the monolayer, 89WP-FAM remained intact in the extracted sample from the basolateral side, testified by fragment ions in ESI-MS spectrum (**Fig. S9C**). Besides, significant cellular uptake of the permeated 89WP-FAM was observed by WERI-Rb-1 cells seeded in the basolateral side (**Fig. S9E, S9F**).

Freshly excised rabbit cornea and sclera were exploited to investigate permeation of Cy5-89WP across the ocular absorption barriers. For Cy5 treated group, nearly no fluorescent signal was observed up to 4 h in cornea or sclera (**Fig. S10**). In contrast, Cy5-89WP was found in corneal epithelium after 1 h treatment, and remained up to 4 h (Fig. 5B **(a)**). Cy5-89WP was also clearly observed in sclera in 1 h, and the permeation depth of Cy5-89WP in sclera demonstrated a five-fold increase from 1 h to 4 h (**Fig. S10B)**.

According to the quantitative results (Fig. 5B **(b)**), Cy5-89WP crossed the excised cornea and sclera in a linear manner within 4 h. After diffusion for 4 h, the cumulative amount of Cy5 in basolateral side was respective 0.27% for cornea and 0.85% for sclera. However, they increased to 1.04% and 6.13% for Cy5-89WP. The P_{app} of Cy5 across cornea and sclera was respective 7.3×10^{-7} cm/s and 2.3×10^{-6} cm/s, while Cy5-89WP demonstrated a 3.8- and 7.4-time increase across cornea and sclera ($p < 0.0001$, Fig. 5B **(c)**). It was also worth noting that the P_{app} of Cy5-89WP across sclera was 7.4 time higher than across cornea.

89WP enabled penetration of the conjugates into the back of eye via a non-corneal pathway. After topical instillation, free FAM or Cy5 solution could hardly be absorbed into the mice eyes, evidenced by no perceptible fluorescence signal in the whole eye balls (Fig. 6A). In contrast, topical instillation of 89WP-FAM and Cy5-89WP into the conjunctival sac led to obvious fluorescent signal, mainly in the posterior ocular segment. According to the semi-quantitative results (Fig. 6B, 6C), the fluorescence intensity of the covalent conjugates in retina peaked at 4 h after instillation with a retention time longer than 24 h. However, there was only little FAM distributed in retina from 2 to 4 h after instillation, and nearly no Cy5 could reach retina. In the retinal sections (**Fig. S11**), the covalent conjugates abundantly accumulated in the periocular tissue during 4 to 18 h, which served as a depot to achieve extended release of conjugates to the retina. These results suggested that 89WP could alternatively facilitate penetration of covalent conjugates into the back of the eye via a non-corneal pathway.

89WP-conjugation strategy was safe for noninvasive intraocular delivery of small molecules. As the eye is a particularly susceptible organ, safety evaluation of 89WP-Mel both *in vitro* and *in vivo* was incredibly important. As shown in Table 2 and **Fig. S12**, the IC_{50} values of 89WP against HCEC, ARPE-19 and WERI-Rb-1 cells were about ≥ 200 μM. The IC_{50} values of 89WP-Mel on normal ocular cells (HCEC and ARPE-19 cells) were about 500 folds higher than that on WERI-Rb-1 cells (0.28 μM). According to the results of the *ex vivo* tissue sections, covalent conjugates did not cause impairment on corneal epithelium and sclera after 4 h incubation (**Fig. S13**). After pharmacodynamical evaluation, the treated cornea and visceral organs were sectioned. No any damage occurred during the long-term treatment (**Fig. S14**, **S15**). Besides, melphalan is insoluble in normal saline (< 1μg/mL) and therefore organic solvents such as propylene glycol and ethanol were needed in the formulations of intraocular injection or eye drops[18]. However, solubility of melphalan in normal saline increased to over 5 mg/mL after conjugated with 89WP, which could allow abolishing irritant organic solvents in the formulation.

Table 2
Solubility of peptide 89WP, melphalan (Mel) and conjugate 89WP-Mel in normal saline, and their half maximal inhibitory concentration (IC_{50}) on different cells.

Compound		89WP	Mel	89WP-Mel
Solubility		54.1 ± 0.98 mg/mL	< 1 μg/mL	5.12 ± 0.30 mg/mL*
IC_{50}	HCEC	199.8 μM	112.8 μM	146.9 μM
	ARPE-19	263.7 μM	200.4 μM	177.4 μM
	WERI-Rb-1	296.9 μM	1.02 μM	0.28 μM
* Solubility of melphalan part in 89WP-Mel.				

Discussion

Advances in chemotherapy have improved the probability of eye salvage for the youths suffering retinoblastoma[4]. However, the clinical administration routes, including intra-artery and intravitreal injections, are difficult to operate with low patient compliance due to indispensable frequent injections[3]. Topical instillation is convenient but still an unmet clinical need for intraocular tumor therapy. Intrinsic defense mechanisms keep most exogenous molecules out of the eye, causing bioavailability of eye drops usually less than 5%. Only trace amount could enter posterior ocular segment[22].

Recently, cell-penetrating peptides are emerging as promising tools for improved ocular drug delivery[23, 24]. In this work, we postulate that penetratin derivative-conjugation strategy may improve absorption of eye drops to achieve effective intraocular concentration of drugs, which are only intravitreally applied before. On a retinoblastoma-bearing mice model, 89WP-Mel demonstrated significantly better intraocular tumor inhibition effects via topical instillation than free melphalan. Besides, the high-dose 89WP-Mel treatment efficiently restricted the proliferation of vitreous seeds and displayed similar tumor inhibition effects compared with intravitreally injected melphalan. According to the results of the immunohistochemical stained sections of mouse brain, the positive signal in spinal trigeminal nucleus revealed the intraocular tumor would metastasize to brain to induce almost 100% mortality. Based on our previous work[16, 17], we considered that “outside-in” absorption of 89WP-Mel would confine the tumor cells inside the eye, while the diffusion of intravitreally injected melphalan compelled the metastases. This hypothesis was further verified by the results of pharmacodynamical evaluation. 89WP-Mel treated mice possessed the highest survival rate and the lowest brain metastases rate (Fig. 3).

The ocular adsorption route of 89WP-Mel was explored to verify the probable anti-metastases mechanism. Conjugation with 89WP ensured substantial increase in cellular uptake of small molecules in HCEC and ARPE-19 cells. However, cellular uptake of the mixture with 89WP displayed no significant difference compared to the free small molecules, suggesting the indispensable role of covalent conjugation in facilitating the uptake of these molecules. Besides, the covalent conjugates entered cells

through an energy-dependent and clathrin-mediated endocytosis pathway, accompanying with an endosomal escape capability enabled by 89WP to further achieve the posterior ocular permeation.

In the *in vitro* models of ARPE-19 cell monolayer, 89WP-FAM exhibited high permeability across the whole monolayer, and could penetrate the monolayer in an intact structure, followed with entry into tumor cells in the bottom chamber. As a hydrophilic molecule, it was difficult for Cy5 to enter into cornea or sclera. In contrast, the permeability of Cy5-89WP dramatically improved, especially in sclera. Cy5-89WP was also endowed with additional adhesive potential on the corneal surface. In other words, topical instillation of Cy5-89WP or other 89WP-engaged conjugates would adhere to the ocular surface, probably due to electrostatic interaction between cationic 89WP and anionic mucin on the ocular surface, and subsequently permeated into the eye mainly through the sclera[25].

By topical instillation, neither hydrophobic FAM nor hydrophilic Cy5 alone could permeate into the eye mainly due to tear turnover, corneal epithelial barrier and other ocular protecting barriers, which was a common absorption challenge for most of eye drops in the market[23, 26]. Both 89WP-FAM and Cy5-89WP exhibited obvious distribution in the posterior ocular segment after topical instillation, but much less distribution in anterior segment, which further confirmed ocular absorption of the covalent conjugates mainly through the non-corneal pathway. In addition, both conjugates could reside in the retina up to 24 h, which was critical to reduce the administration frequency.

Taken together, conjugation with 89WP firmly improved ocular absorption of small molecules, especially in the posterior segment mainly through a non-corneal pathway. As shown in Fig. 7, we deduced that such “outside-in” absorption manner of topically instilled 89WP-Mel created a protective shield surrounding the whole eye, which killed tumor cells in a “siege” way and therefore would efficiently prevent extraocular tumor metastases, either via optic nerve or the circulating subarachnoid fluid tumor cells[27]. In contrast, although with almost 100% drug bioavailability, the “inside-out” diffusion made intravitreally injected melphalan kill tumor cells in a “pursuit” way, which might weaken the efficiency on distant tumor cells and even “facilitate” tumor metastases.

Considering melphalan is a cytotoxic agent, biosafety for ocular application is also important for the druggability[28]. In cytotoxicity evaluation, the IC_{50} values of 89WP-Mel on HCEC and ARPE-19 cells were ≥ 500 times more than that on WERI-Rb-1 cells. When the concentration of melphalan was 1-100 μM, 89WP-Mel exhibited nearly no toxicity on HCEC and ARPE-19 cells, but the survival rate of WERI-Rb-1 cells was lower than 50%. Compared to tumor cells WERI-Rb-1, normal ocular cells HCEC and ARPE-19 were relatively low proliferative and would be much less sensitive to melphalan[29, 30]. In addition, there was also no obvious tissue injury occurred caused by topical instillation of 89WP-Mel. Due to low solubility of melphalan, the marketed product contains propylene glycol and ethanol in solvent, which might induce the ocular irritation during long-term use[18, 31]. Conjugation with hydrophilic 89WP could increase the solubility of melphalan more than 5000 times in physiological saline, implying that 89WP-Mel could be dissolved in aqueous media as eye drops for intraocular tumor inhibition at a concentration over 5.0 mg/mL (melphalan) without the need of any other co-solvent.

Conclusions

In the present work, melphalan was successfully conjugated with a specially designed ocular permeation enhancer 89WP without impairing the antineoplastic activity. Topical instillation of 89WP-Mel was proven as a safe and efficient anti-retinoblastoma treatment, which exhibited not only the significant improvement in infant compliance but also additional advantages over intravitreally injection, especially in preventing brain metastases. The probable mechanism was related to the enhanced ocular absorption and the “outside-in” absorption manner of 89WP-Mel. Besides, conjugation with hydrophilic 89WP increased the solubility of insoluble molecules such as melphalan, which make it possible that the chemotherapeutics could be administered as an ophthalmic solution. Taken together, 89WP-conjugation strategy could change intraocular injections of various small molecules to much safer eye drops, also providing an alternative approach on the treatment of metastatic intraocular diseases.

Materials And Methods

Materials

Peptides 89WP (RQIKIWFWWRRMKWKK), N-terminal cysteine capped 89WP (Cys-89WP, CRQIKIWFWWRRMKWKK) and C-terminal FAM-labeled 89WP (89WP-FAM, RQIKIWFWWRRMKWKKK-FAM) were synthesized by Kangbeibio (Ningbo, China). Hydrophilic cyanine-5 maleimide derivative (sulfo-Cy5-Mal) was purchased from Ruixi Biological Technology (Xi’an, China). Fmoc-protected α-amino acids were from GL Biochem (Shanghai, China). Wang resin (Substitution = 0.54 mmol/g) was from Xi'an Innovision Bioscience (Xi'an, China). Fmoc N-hydroxysuccinimide ester (Fmoc-OSu), N,N’-diisopropylcarbodiimide (DIC), 4-dimethylaminopyridine (DMAP), O-benzotriazole-N,N,N',N'-tetramethyl-uronium-hexafluorophosphate (HBTU), 1-Hydroxybenzotriazole anhydrous (HOBT) and N,N-diisopropylethylamine (DIEA) were purchased from Aladdin Reagent (Shanghai, China). Fetal bovine serum (FBS), Dulbecco’s Modified Eagle Medium (DMEM), DMEM/Nutrient Mixture F-12 (DMEM/F12), Roswell Park Memorial Institute 1640 Medium (RPMI 1640), antibiotics (Penicillin-Streptomycin, 10,000 U/mL) and LysoTracker™ Red DND-99 were purchased from Thermo Fisher (Massachusetts, United States). Melphalan, 3-(4,5-dimethylthiazol-2-yl)-2,5-diphenyltetrazolium bromide (MTT), Cell Counting Kit-8 (CCK-8) and 4,6-diamidino-2-phenylindole (DAPI) were from Dalian Meilun Biotechnology (Dalian, China). All the other reagents used in this work were of analytical grade, except chromatographic grade for liquid chromatography.

Cell cultivation

Human corneal epithelial cells (HCEC, BNCC337876) and Human umbilical vein endothelial cells (HUVEC, ATCC® CRL-1730™) were cultivated in DMEM medium supplemented with 10% FBS and 1% antibiotics at 37°C in a 5% CO_2 humidified atmosphere. Human retinal pigment epithelial cells (ARPE-19, GNHu45) were cultivated in DMEM/F12 medium supplemented with 10% FBS and 1% antibiotics at 37°C in a 5% CO_2 humidified atmosphere. Human retinoblastoma cells (WERI-Rb-1, TCHu213) and Fluc/GFP-Rb-1 cells

were cultured in RPMI-1640 medium supplemented with 10% FBS and 1% antibiotics at 37°C in a 5% CO_2 humidified atmosphere. ARPE-19 and WERI-Rb-1 cells were kindly provided by Stem Cell Bank, Chinese Academy of Sciences. Fluc/GFP-Rb-1 cells were obtained in our previous work[16].

Animals

Animals used in this work were obtained from the Experimental Animal Center of Fudan University and maintained at 22 ± 2°C on a 12 h light–dark cycle with access to food and water *ad libitum*. The animals for the experiments were treated according to protocols that were evaluated and approved by the Ethical Committee of Fudan University, and were acclimatized to laboratory conditions for 1 week prior to experiments.

Synthesis, purification and characterization

Conjugation of 89WP and hydrophilic Cy5 was through Michael addition reaction of thiol and maleimide. Briefly, Cys-89WP was mixed with sulfo-Cy5-Mal (1.2 eq.) in 10 mM phosphate buffer (PB, pH7.2) under nitrogen protection and stirred overnight at room temperature. Purification was implemented via Pre-HPLC (Waters, United States) on a reversed-phase C_{18} column (Waters, United States). The conjugate Cy5-89WP was obtained with a further freeze-drying process, and characterized by HPLC (Agilent, United States) and ESI-MS (AB, United States). An ODS column (YMC, 4.6 × 150 mm, 5 μm) was used at 25°C for HPLC analysis. The mobile phase was acetonitrile (0.1% trifluoroacetic acid, TFA):distilled water (0.1% TFA) at 5%–65% gradient in 30 min, at a flow rate of 0.7 mL/min. UV absorbance of the effluent was monitored at 214 nm. In ESI-MS analysis, the mobile phase was methanol (80%):distilled water (19.9%):formic acid (0.1%), at a flow rate of 0.3 mL/min, capillary voltage was 3000 V, and flow rate of drying gas at the temperature of 350°C was 12 L/min. Cysteine was conjugated to sulfo-Cy5-Mal using above method to obtain hydrophilic Cy5-Cys (abbreviating to Cy5 in this work).

Solid phase synthesis was used to accomplish conjugation of 89WP and melphalan (89WP-Mel) using Wang resin according to Fmoc methodology. Fmoc-protected melphalan (Fmoc-Mel) was synthesized via mixing melphalan (1.0 eq.) with Fmoc-OSu (1.2 eq.) in dioxane at 50°C with agitation overnight. The mixture was directly used for next procedure after the solvent dried under vacuum. Fmoc-Mel was added to Wang resin (0.5 eq.) after 5 min of pre-activation in dichloromethane (DCM) using DMAP (1.2 eq.) and DIC (1.0 eq.) as catalysts. After washing with dimethylformamide (DMF), acetic anhydride (5.0 eq.) and pyridine (5.0 eq.) were introduced to block unreacted active sites of the resin. The resin was immersed in piperidine/DMF (2:8) solution for 15 min twice to remove Fmoc-group and then rinsed with DMF. Further peptide condensation was facilitated by using excess Fmoc-protected amino acid (8.8 eq. to Wang resin, similarly hereinafter) activated with HBTU (8.8 eq.), HOBT (8.8 eq.) and DIEA (17.6 eq.) for 1 h in DMF. The Fmoc deprotection was implemented as above. The resin bound 89WP-Mel was rinsed 3 times with DMF and 3 times with DCM/methanol (1:1), and dried under vacuum. The conjugate 89WP-Mel were deprotected and cleaved from resin with a cocktail mixture (9.5 mL of TFA, 0.25 mL of triisopropylsilane and 0.25 mL of H_2O, per 1.0 g of resin) for 3 h at room temperature. The resulting solution was

concentrated to an oil in vacuo and cold diethyl ether was poured over the solutions to precipitate the samples. Purification and characterization of 89WP-Mel were similar with Cy5-89WP.

Cellular uptake, endocytosis mechanism and cytotoxicity

For quantitative cellular uptake evaluation of conjugates, HCEC or ARPE-19 cells cultivated on 24 well plates at a primary density of 20,000 cells/well were incubated with FAM, mixture of 89WP and FAM, or 89WP-FAM for 4 h, and all of them contained 3 μM FAM. After washed with 10 mM PBS containing 0.02 mg/mL heparin sodium three times and trypsinized, the cells were resuspended in 10 mM PBS, and the amount of FAM-positive cells and mean fluorescence intensity were tested by flow cytometer (BD, United States). The cells were also incubated with Cy5, mixture of 89WP and Cy5, or Cy5-89WP and tested as above. The concentration of Cy5 was 3 μM.

To discern conjugates 89WP-FAM and Cy5-89WP distribution in HCEC or ARPE-19 cells, each cells cultivated on 35mm 4-chamber glass bottom dishes at a primary density of 20,000 cells/well were incubated with related molecules for 4 h, respectively. Then the cells were washed with 10 mM PBS containing 0.02 mg/mL heparin sodium and immersed in glycerine/10 mM PBS (1:1, volume ratio) for further observation under confocal laser scanning microscope (Carl Zeiss, Germany).

To identify probable internalization mechanisms of 89WP-engaged conjugates, ARPE-19 cells were pre-incubated at 4°C or treated with inhibitors at 37°C for 0.5 h, then incubated with the 89WP-FAM at 4°C or in the presence of inhibitors at 37°C for another 1.5 h. The cellular uptake of 89WP-FAM at 37°C was used as the positive control (100% uptake efficiency). The results are shown as relative uptake rate of different groups normalized according to the positive control.

Endosomal escape ability of 89WP-engaged conjugates was evaluated via an erythrocyte lysis assay[32]. Briefly, freshly prepared human erythrocytes were resuspended in sodium citrate buffer (300 mM NaCl, 30 mM sodium citrate) at a concentration of 7×10^7 cells/mL, following incubation with equal volume of 89WP solution at a series of concentrations for 1 h at 37°C. After centrifugation (1000 g × 5 min), 100 μL of the supernatant were transferred to a 96-wells plate and $OD_{450\ nm}$ was determined via microplate reader (Bio-Tek, United States). The distilled water was used as the negative control (no hemolysis) while 10% Triton X-100 solution was used as the positive control (100% hemolysis).

HCEC, ARPE-19 or WERI-Rb-1 cells at the logarithmic growth phase were cultivated on 96 well plates at a primary cell density of 2,000 cells/well for 24 h. Cells were then incubated with 89WP, melphalan or 89WP-Mel at concentration gradients for 4 h, following a further cultivation in 200 μL complete medium for 20 h except WERI-Rb-1 cells. After that, cells were incubated with 0.5 mg/mL MTT reagent in each well for 4 h at 37°C, and produced formazan was dissolved in 150 μL DMSO, except that WERI-Rb-1 cells were treated with CCK-8 reagent for 2 h after incubation with 89WP-Mel. The OD_{490} was measured via microplate reader.

Transport efficiency across *in vitro* ARPE-19 cell monolayer

The *in vitro* ARPE-19 cell monolayer model was established as previously reported with slight changes[21]. Briefly, ARPE-19 cells were seeded on the front of rat tail collagen type Ⅰ coated 6.5 mm polyester membrane filters (pore size 0.4 μM, Corning) at a density of 5,000 cells/well, respectively. Transepithelial electrical resistance (TEER) was measured by an epithelial volt-Ωm (Millipore, USA) to confirm the barrier integrity. Monolayers with TEER over 100 $\Omega \cdot cm^2$ were chosen for the further experiments. The apical side of monolayers was incubated with FAM, mixture of 89WP and FAM, or 89WP-FAM in 100 μL D-Hanks balanced salt solution (D-HBSS, pH7.2) while the basolateral side was 600 μL D-HBSS. All of three groups contained FAM at a concentration of 3 μM. An aliquot of 200 μL of sample was extracted from the basolateral side every 0.5 h, and followed with addition of 200 μL fresh D-HBSS. Fluorescence intensity of the extracted sample was measured via microplate reader. Post-transported monolayers were also observed under confocal laser scanning microscope. To evaluate permeability of the conjugate, the apparent permeability coefficient (P_{app}, $cm \cdot s^{-1}$) was calculated as previously reported[11]. The samples in acceptor side were also characterized by HPLC and ESI-MS after a dialysis (MWCO 1000 Da) and freeze-drying process. The HPLC and ESI-MS conditions were same as mentioned above.

In another monolayer model, the acceptor side was seeded with WERI-Rb-1 cells at a density of 20,000 cells/well in RMPI 1640 medium. The FAM and 89WP-FAM in DMEM/F12 medium were added into the apical side and incubated for 4 h at 37°C. Then the WERI-Rb-1 cells were collected for flow cytometry analysis.

Ex vivo corneal and scleral permeability

Permeability of the Cy5-89WP through excised rabbit cornea and sclera was evaluated using horizontal diffusion cells as previously reported[11]. Animals were euthanized by an overdose of sodium pentobarbital (150 mg/kg) administered through marginal ear vein. Then the cornea and sclera were excised and immediately transferred into normal saline. Each cornea or sclera was placed vertically between the diffusion cells with epithelium orienting to the donor cells. Both donor and acceptor cells contained 3.5 mL normal saline as the diffusion medium, which was maintained at 34 ± 0.5°C by circulating water bath, and 5 μM Cy5 or Cy5-89WP was added in the donor side, respectively. An aliquot of 500 μL of sample was extracted from the acceptor cell every 0.5 h for 4 h, and followed with supplement of 500 μL fresh normal saline. Fluorescence intensity of the samples was measured via microplate reader. To compare *ex vivo* tissue permeability of Cy5 and Cy5-89WP, the apparent permeability coefficients (P_{app}, $cm \cdot s^{-1}$) were calculated as mentioned above.

After the diffusion, the cornea and sclera were fixed in 4% paraformaldehyde, dehydrated in 30% sucrose solution and dyed with hematoxylin-eosin or DAPI for further observation by microscope.

Intraocular distribution and pharmacokinetics

Male mice (18 ~ 20 g) derived from Institute of Cancer Research, United States were used in this experiment. Both 30 μM 89WP-FAM and Cy5-89WP dissolved in 10 μL artificial tear fluid[33] were instilled

into the conjunctival sac of mice, respectively. After instillation, the mice were sacrificed (injection with the fatal dose of pentobarbital sodium, 150 mg/kg) 0.5 h, 2 h, 4 h, 8 h, 12 h, 18 h, 24 h later and the eyeballs were fixed in Davidson's solution for 0.5 h, following an overnight dehydration in 30% sucrose. DAPI-stained frozen sections were observed under an inverted fluorescence microscope (Leica, Germany).

Inhibition of intraocular retinoblastoma via topical instillation

Intraocular tumor-bearing mice model were established as previously reported[16]. Briefly, the male Balb/c nude mice were anesthetized by intraperitoneal injection with pentobarbital sodium (30 mg/kg) in combination with topical application of 0.4% oxybuprocaine hydrochloride. Topical instillation of 0.5% tropicamide was used to dilate the pupil. Fluc/GFP-Rb-1 cells (2×10^4 cells suspended in 2 μL 10 mM PBS) were injected slowly into the vitreous body near retina of the right eye using a microsyringe (33 G, Hamilton), following instillation of 0.25% chloramphenicol. Ocular luminescence of the mice was detected in the following days and the tumor-bearing mice were randomly divided into five groups (n = 5) in the first evaluation and four groups in the second evaluation (n = 8).

In the first evaluation (safety and preliminary pharmacodynamics evaluation), mice were treated with 10 μL of normal saline (N.S.), melphalan (3.0 mg/mL, dissolved in a cocktail of 1, 2-propanediol, ethyl alcohol, sodium citrate and distilled water), 89WP-Mel (containing melphalan 0.3 or 3.0 mg/mL, dissolved in normal saline) via topical instillation once daily from Day 0 to Day 30. Intravitreal injection of melphalan (8.0 mg/mL in 2 μL cocktail mentioned above, once a month) was used as the positive control. After 1-month treatment, the mice were sacrificed (injection with the fatal dose of pentobarbital sodium, 150 mg/kg) and the treated eyes and visceral organs were fixed in 4% paraformaldehyde, dehydrated in 30% sucrose solution and dyed with hematoxylin-eosin (HE) for further observation under microscope. Brain from a survival mouse in topically instilled melphalan group was also treated as above and implemented immunohistochemical experiments using HRP-labeled anti-GFP primary antibody (ab183734, Abcam) for metastasizing tumor cells detection.

In the second evaluation (optimized pharmacodynamics evaluation), mice were treated with 10 μL of normal saline, melphalan (3.0 mg/mL), 89WP-Mel (containing melphalan 3.0 mg/mL) via topical instillation once daily from Day 0 to Day 60. Intravitreal injection of melphalan (0.5 mg/mL in 2 μL medium composed of 10% cocktail and 90% N.S.) once on alternate weeks was used as the positive control. The mice were intraperitoneal injected with 150 mg/kg D-luciferin and anesthesia by isoflurane 15 min before luminescence signal was detected via the IVIS Spectrum system (PerkinElmer, USA). *In vivo* imaging was carried out on Day 0, 2, 4, 6, 9, 12, 15, 17, 20, 25, and 30. When the mice was moribund (body weights fast decreased to lower than 21 g) or at the end of experiment (Day 60), the whole brain of sacrificed mice was fixed in 4% paraformaldehyde, dehydrated in 30% sucrose solution and was implemented immunohistochemical experiments using HRP-labeled anti-GFP primary antibody (ab183734, Abcam) for metastasizing tumor cells detection.

Statistical analysis

Statistical significances of the quantitative data were analyzed by the One-way ANOVA multiple comparison or t-test. Considered that $p > 0.05$ was no significant, $p < 0.05$ was significant, and $p < 0.01$ even $p < 0.001$ was highly significant.

Declarations

Date availability

The data that support the findings of this study are available within the paper and the Supplementary Information. All other data are available from the authors upon reasonable request.

Acknowledgments

We are grateful for the financial support from the Shanghai Science and Technology Program (21ZR1407100 and 21S11905300 to G. W.), National Natural Science Foundation of China (81573358 to G. W., 81673361 to C. Z., and 81690263 to W. L.), China Postdoctoral Science Foundation (2020TQ0081 to K. J.) and Development Project of Shanghai Peak Disciplines-Integrative Medicine (20180101 to G. W.).

Author contributions

G. W. and C. Z. conceived and designed this research; K. J. contributed to animal experiments, data presentation and manuscript preparation; X. F. performed synthesis of conjugates and safety evaluation; Y. H. and S. Y. performed cellular experiments; W. L. and Y. L. contributed to data interpretation.

Competing interests

The authors declare no competing financial interest.

References

1. Dimaras, H. et al. Retinoblastoma. *Lancet.* **379**, 1436–1446 (2012).
2. Dimaras, H. et al. Retinoblastoma. *Nat. Rev. Dis. Primers.* **1**, 15021(2015).
3. Yanık, Ö. et al. Chemotherapy in retinoblastoma: Current approaches. Turk. J. Ophthalmol. **45**, 259–267 (2015).
4. Fabian, I. D. et al. The management of retinoblastoma. *Oncogene.* **37**, 1551–1560 (2018).
5. Singh, A. D. Retinoblastoma: What is the future? *Int. Ophthalmol. Clin.* **59**, 95–99 (2019).
6. Mendoza, P. R. et al. Therapeutic options for retinoblastoma. *Cancer Control.* **23**, 99–109 (2016).
7. Manjandavida, F. P. et al. Intra-arterial chemotherapy in retinoblastoma - A paradigm change. *Indian J. Ophthalmol.* **67**, 740–754 (2019).
8. Yousef, Y. A. et al. Intravitreal melphalan chemotherapy for vitreous seeds in retinoblastoma. *J. Ophthalmol.* 2020, 8628525 (2020).

9. Ghassemi, F. et al. Risk definition and management strategies in retinoblastoma: Current perspectives. *Clin. Ophthalmol.* **9**, 985–994 (2015).
10. Buitrago, E. et al. Pharmacokinetics of melphalan after intravitreal injection in a rabbit model. *J. Ocul. Pharmacol.* **32**, 230–235 (2016).
11. Liu, C. et al. Penetratin, a potentially powerful absorption enhancer for noninvasive intraocular drug delivery. *Mol. Pharm.* **11**, 1218–1227 (2014).
12. Jiang, K. et al. Inhibition of post-trabeculectomy fibrosis via topically instilled antisense oligonucleotide complexes co-loaded with fluorouracil. *Acta Pharm. Sin. B.* **10**, 1754–1768 (2020).
13. Liu, C. et al. Facile noninvasive retinal gene delivery enabled by penetratin. *ACS Appl. Mater. Inter.* **8**, 19256–19267 (2016).
14. Tai, L. et al. A novel penetratin-modified complex for noninvasive intraocular delivery of antisense oligonucleotides. *Int. J. Pharm.* **529**, 347–356 (2017).
15. Tai, L. et al. Noninvasive delivery of oligonucleotide by penetratin-modified polyplexes to inhibit protein expression of intraocular tumor. *Nanomedicine.* **13**, 2091–2100 (2017).
16. Jiang, K. et al. Octopus-like flexible vector for noninvasive intraocular delivery of short interfering nucleic acids. *Nano Lett.* **19**, 6410–6417 (2019).
17. Jiang, K. et al. Discerning the composition of penetratin for safe penetration from cornea to retina. *Acta Biomater.* **63**, 123–134 (2017).
18. Shah, N. V. et al. Intravitreal and subconjunctival melphalan for retinoblastoma in transgenic mice. *J. Ophthalmol.* 2014, 829879 (2014).
19. Weng, Y. et al. Nanotechnology-based strategies for treatment of ocular disease. *Acta Pharm. Sin. B.* **7**, 281–291 (2017).
20. Guan, S. et al. Self-assembled peptide–poloxamine nanoparticles enable in vitro and in vivo genome restoration for cystic fibrosis. *Nat. Nanotechnol.* **14**, 287–297 (2019).
21. Fernandez-Godino, R. et al. Isolation, culture and characterization of primary mouse RPE cells. *Nat. Protoc.* **11**, 1206–1218 (2016).
22. Kang-Mieler, J. J. et al. Advances in ocular drug delivery: Emphasis on the posterior segment. *Expert Opin. Drug Del.* **11**, 1647–1660 (2014).
23. Pescina, S. et al. Cell penetrating peptides in ocular drug delivery: State of the art. *J. Controlled Release.* **284**, 84–102 (2018).
24. Mandal, A. et al. Ocular delivery of proteins and peptides: Challenges and novel formulation approaches. *Adv. Drug Deliver. Rev.* **126**, 67–95 (2018).
25. Li, J. et al. Montmorillonite/chitosan nanoparticles as a novel controlled-release topical ophthalmic delivery system for the treatment of glaucoma. *Int. J. Nanomedicine.* **13**, 3975–3987 (2018).
26. Jumelle, C. et al. Advances and limitations of drug delivery systems formulated as eye drops. *J. Controlled Release.* **321**, 1–22 (2020).

27. Ji X, et al. Noninvasive visualization of retinoblastoma growth and metastasis via bioluminescence imaging[J]. *Invest. Ophthalmol. Vis. Sci.* **50**, 5544–5551 (2009).
28. Xue, K. et al. Ocular toxicity of intravitreal melphalan for retinoblastoma in Chinese patients. *BMC Ophthalmol.* **19**, 61 (2019).
29. Süsskind, D. et al. Toxic effects of melphalan, topotecan and carboplatin on retinal pigment epithelial cells. *Acta Ophthalmol.* **94**, 471–478 (2016).
30. Li, J. et al. Biodegradable reduction-responsive polymeric micelles for enhanced delivery of melphalan to retinoblastoma cells. *Int. J. Biol. Macromol.* **141**, 997–1003 (2019).
31. Day, R. et al. Liquid laundry detergent capsules (PODS): a review of their composition and mechanisms of toxicity, and of the circumstances, routes, features, and management of exposure. *Clin. Toxicol. (Phila).* **57**, 1053–1063 (2019).
32. Plank, C. et al. The influence of endosome-disruptive peptides on gene transfer using synthetic virus-like gene transfer systems. *J. Biol. Chem.* **269**, 12918–12924 (1994).
33. Lorentz, H. et al. Contact lens physical properties and lipid deposition in a novel characterized artificial tear solution. *Mol. Vis.* **17**, 3392–3405 (2011).

Figures

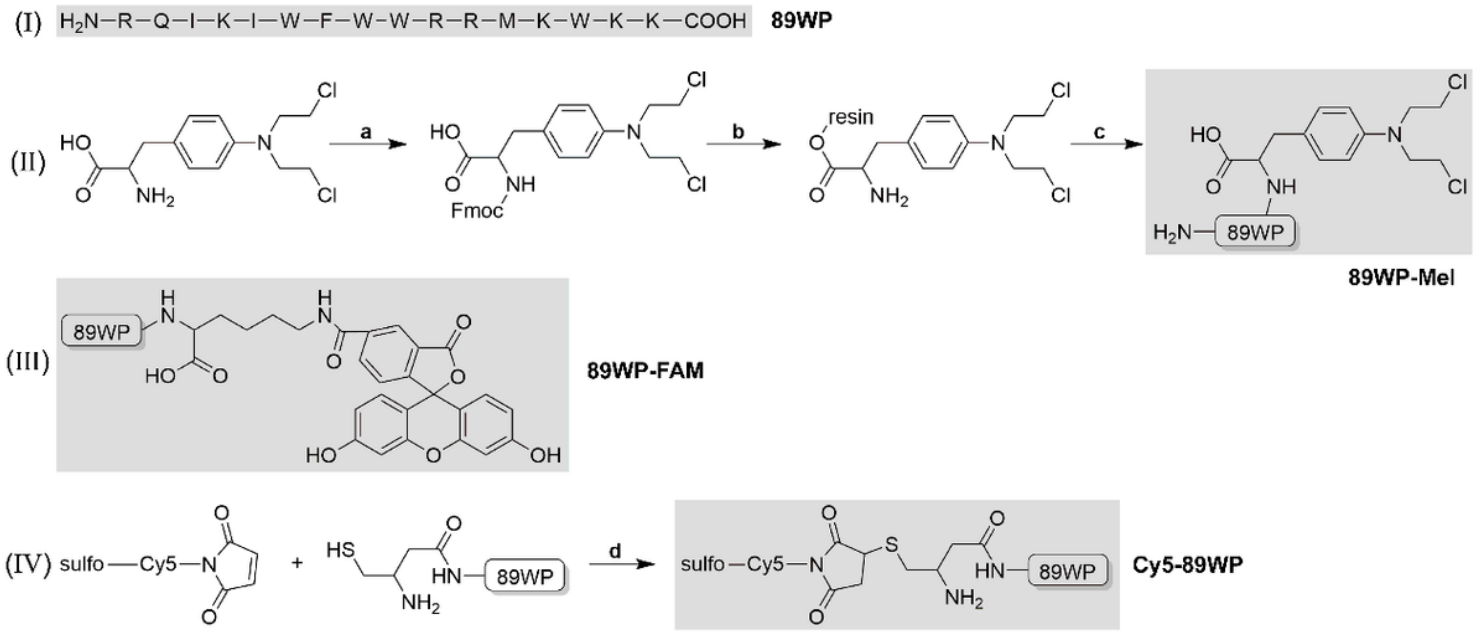

Figure 1

Molecular structure and synthetic routes of conjugates. 89WP and 89WP-FAM were obtained through the commercial way. Reaction conditions in synthesis of 89WP-Mel and Cy5-89WP were as following: a, Fmoc-OSu 1.2 eq. (compared to melphalan), dioxane, 50°C, overnight. b, 1) Wang resin 0.5 eq., DMAP 1.2 eq., DIC 1.0 eq., CH2Cl2, 37°C, 24 h; 2) acetic anhydride 5.0 eq., pyridine 5.0 eq., CH2Cl2, 37°C, 1 h; 3)

piperidine/DMF (2 : 8), 37°C, 15 min, twice. c, 1) Fmoc-amino acid 4.4 eq., HBTU 4.4 eq., HOBT 4.4 eq., DIEA 8.8 eq., 37°C, 1 h; 2) piperidine/DMF (2 : 8), 37°C, 15 min, twice; 3) TFA : TIS : H2O (95 : 2.5 : 2.5), r.t. 3 h; c 3) was implemented after c 1)-c 2) cycle to complete peptide 89WP synthesis. d, N2, 10 mM phosphate buffer, dark, r.t., overnight.

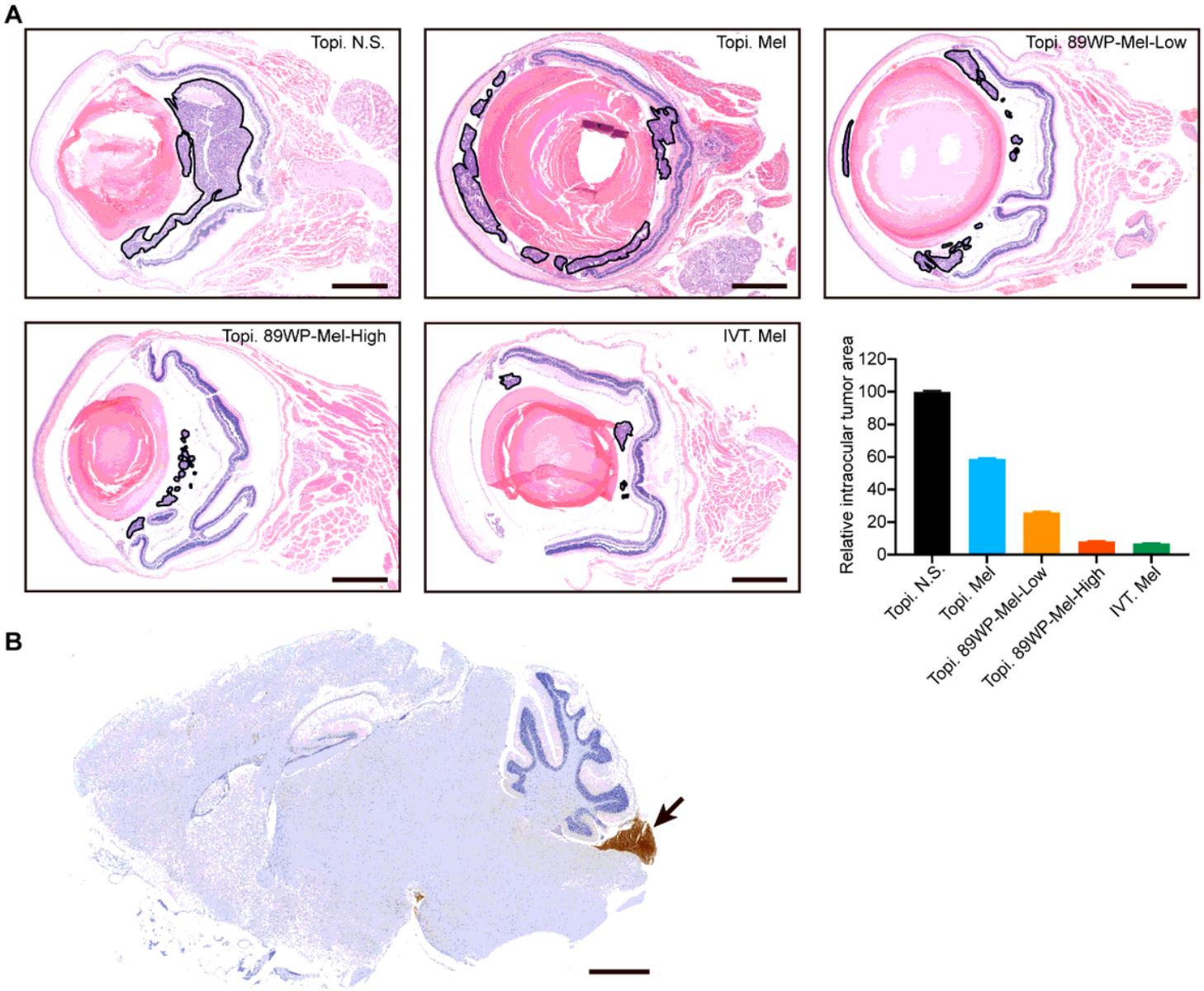

Figure 2

Intraocular tumor proliferation and brain metastases of retinoblastoma-bearing mice at treatment ending. A, Hematoxylin-eosin stained sections of eyes from the mice received 1-month treatment. The tumor regions (vitreous seeds) were circled by black line, with comparing the area calculated by ImageJ software. Scale bar, 0.5 mm. B, Immunohistochemical section of brain from a surviving mouse in topically instilled melphalan treated group. The black arrow pointed the spinal trigeminal nucleus region with positive signal. The primary antibody specifically bound to green fluorescent protein (GFP) in Fluc/GFP-Rb-1 cells. Scale bar, 1 mm.

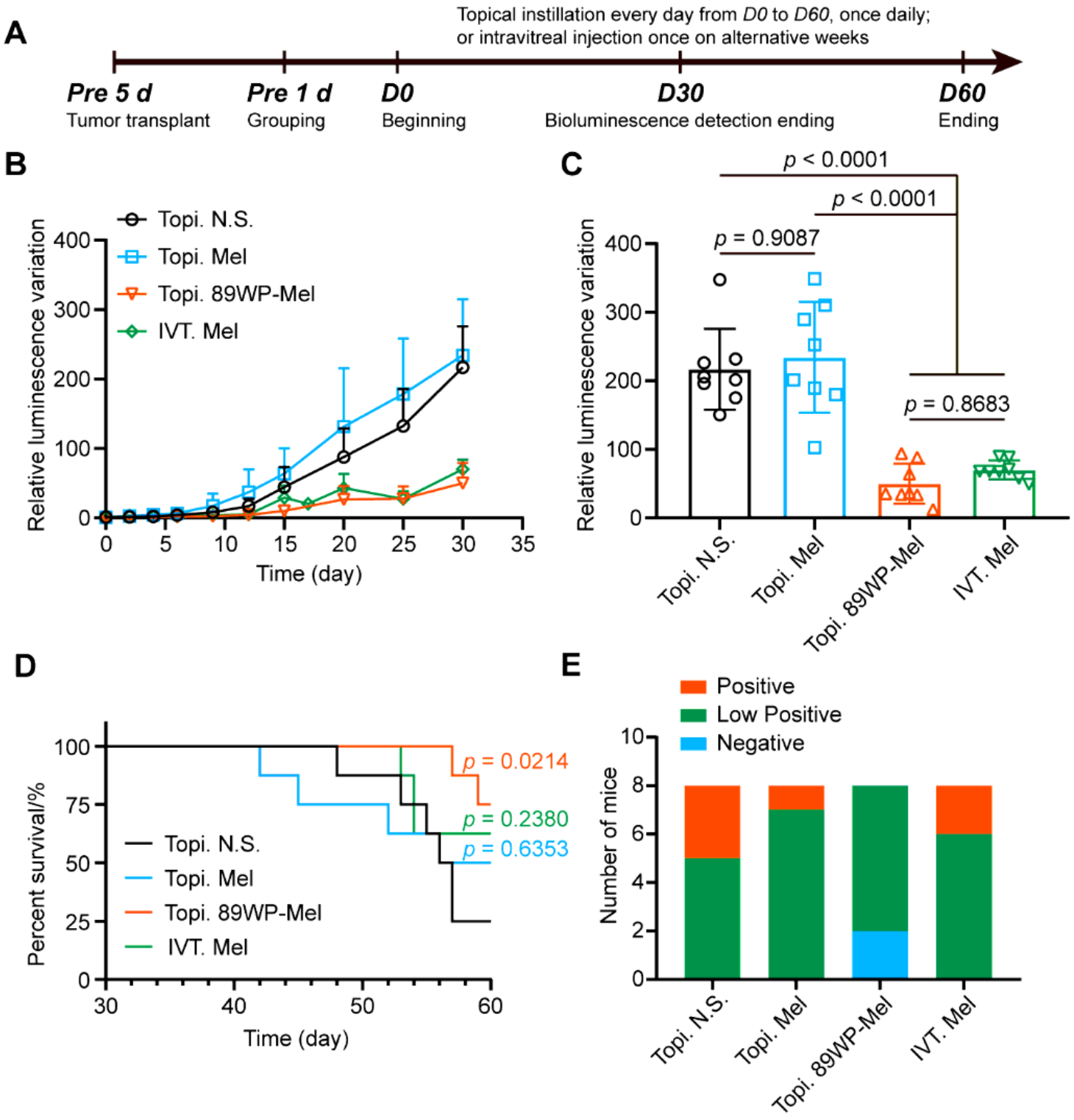

Figure 3

Anti-retinoblastoma effects of 89WP-Mel. A, Time schedule of treatment and evaluation on tumor-bearing mice. B, Intraocular tumor proliferation curves of mice receiving different treatments. The data were shown as increasing folds compared to the initial mean bioluminescence intensity. C, Comparison of intraocular tumor proliferation extent among different groups on the Day 30 during treatments. The statistical significance was analyzed by One-way ANOVA multiple comparisons corrected by Tukey's test (n = 8). D, Survival curves of the treated mice. The statistical significance was analyzed by Survival Curve

comparison corrected by Log-rank (Mantel-Cox) test (compared to the Topi. N.S. group). E, Comparison of brain metastases extent among different groups at treatment ending. The metastases grading (Positive, Low Positive, Negative) was evaluated based on sections in Fig. S5.

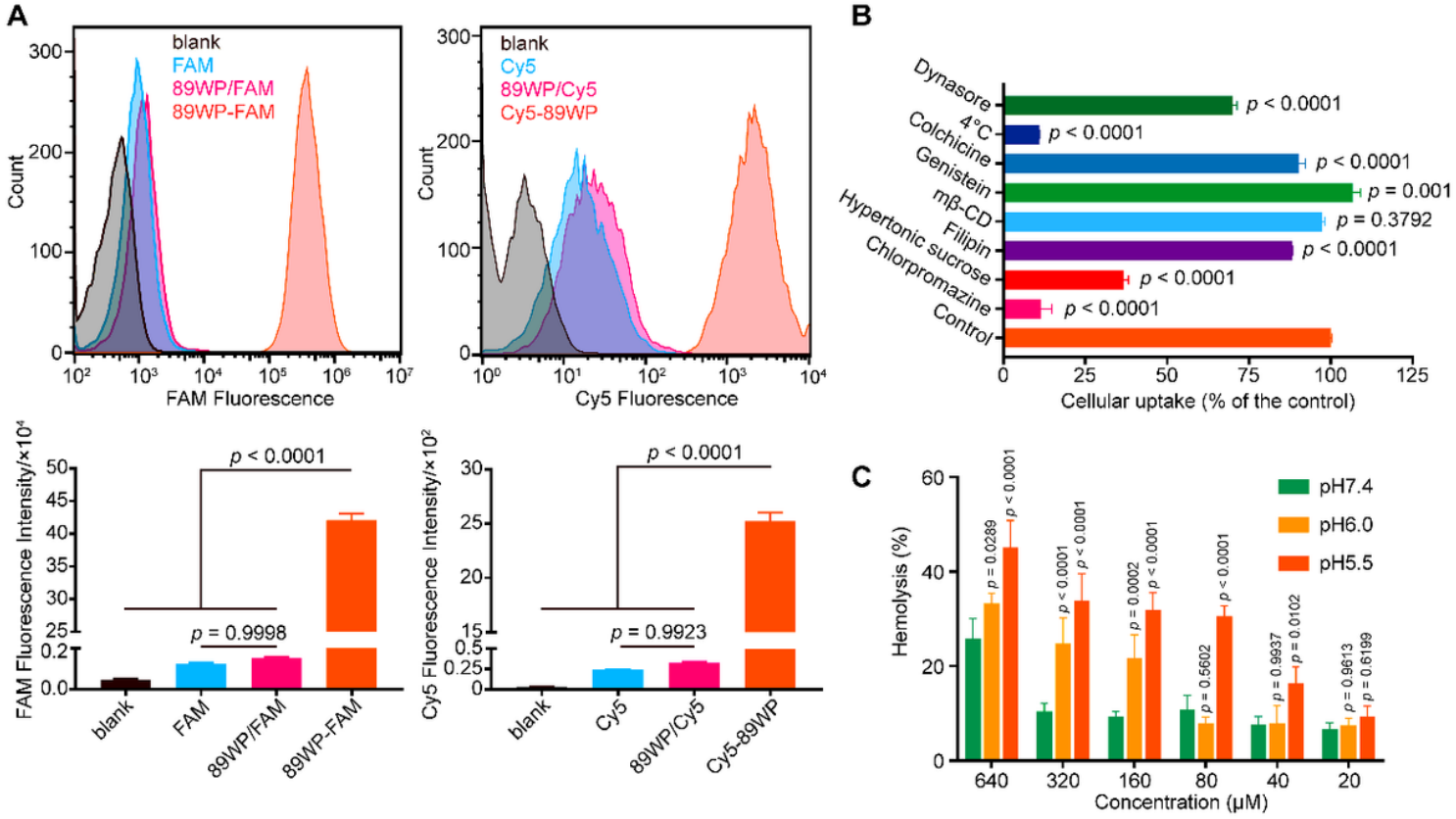

Figure 4

Cellular uptake and endocytic pathways of covalent conjugates of 89WP and small molecules. A, Flow cytometry analysis and the histogram plot of the mean fluorescence intensity in ARPE-19 cells. The cells were treated with 3 μM conjugates for 4 h at 37°C. One-way ANOVA multiple comparisons corrected by Tukey's test was used to determine the statistical significance (n = 3). B, Effects of temperature and endocytosis inhibitors on cellular uptake of 89WP-FAM in ARPE-19 cells. The non-inhibited internalization of 89WP-FAM was used as a positive control (100%). One-way ANOVA multiple comparisons corrected by Dunnett's test was used to determine the statistical significance (n = 3). C, The pH-responsive behavior of 89WP-FAM using hemolysis assay. Isotonic sodium citrate buffer solution was used as a negative control (No hemolysis), and 10% Triton X-100 in incubation medium was used as a positive control (100% hemolysis). Two-way ANOVA multiple comparisons corrected by Tukey's test was used to determine the statistical significance (n = 3, compared with hemolysis ratio of the same concentration of 89WP at pH 7.4).

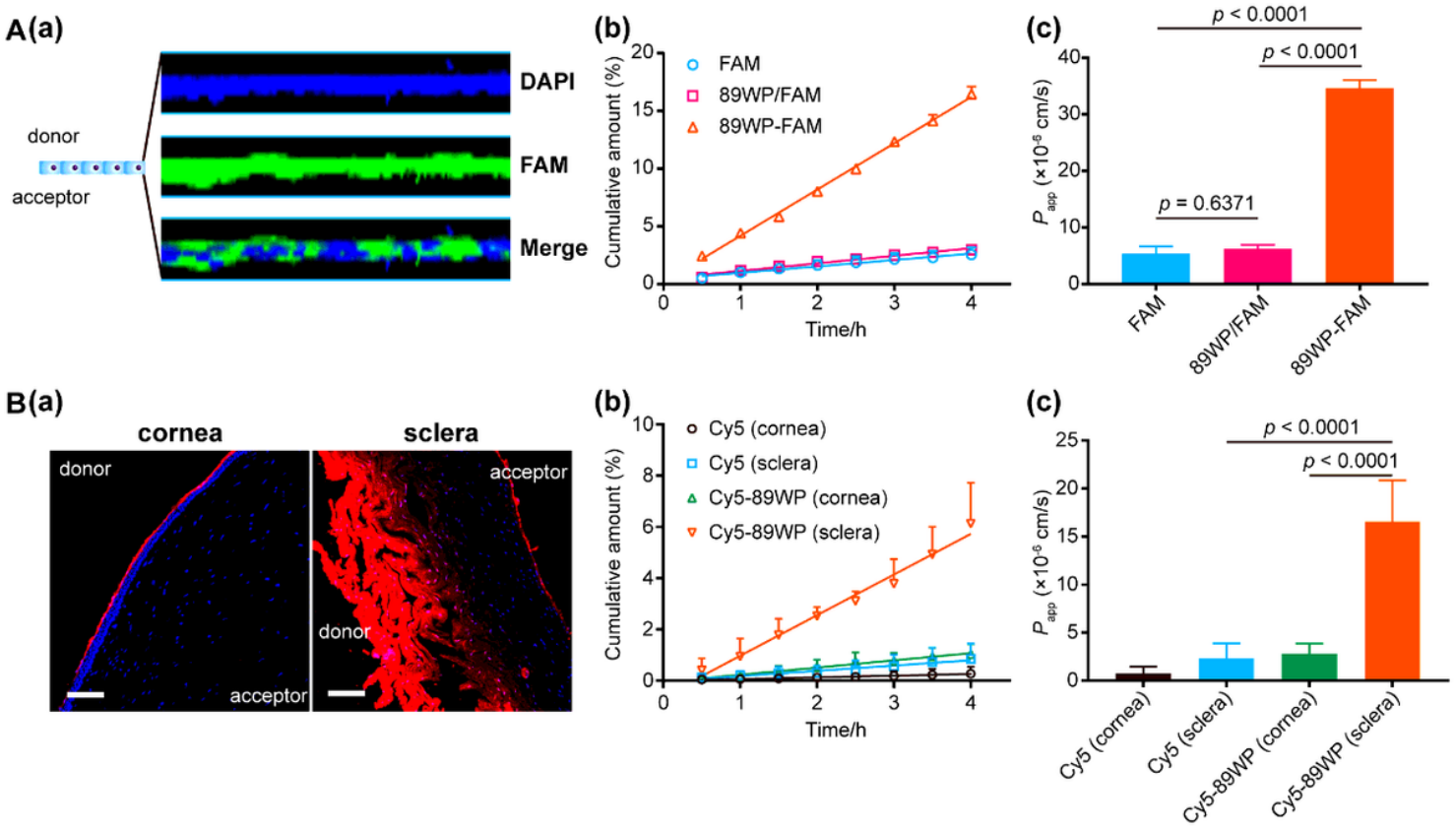

Figure 5

Permeation of 89WP conjugates across the ocular absorption barriers. A, Permeation of 89WP-FAM across the in vitro ARPE-19 cell monolayer. (a), 89WP-FAM (green) permeation depth across the monolayer. The nuclei were stained with DAPI (blue). (b), Cumulative amount of transported FAM or 89WP-FAM in the basolateral side. (c), Apparent permeability coefficient (Papp, cm/s) of FAM and 89WP-FAM across the monolayer. One-way ANOVA multiple comparisons corrected by Tukey's test was used to determine the statistical significance (n = 3). The monolayer was treated with solutions containing 3 μM FAM or 89WP-FAM for 4 h at 37°C. B, Permeation of Cy5-89WP across the ex vivo rabbit cornea and sclera. (a), Distribution of the permeated Cy5-89WP (red) in cornea and sclera after diffusion for 4 h. (b), Cumulative amount of the transported Cy5 or Cy5-89WP across the tissues. (c), Papp of Cy5 and Cy5-89WP across the tissues. The statistical significance was analyzed by One-Way ANOVA multiple comparisons corrected by Tukey's test (n = 3). The tissues were treated with 5 μM Cy5 or Cy5-89WP in the donor side at 34 ± 0.5°C.

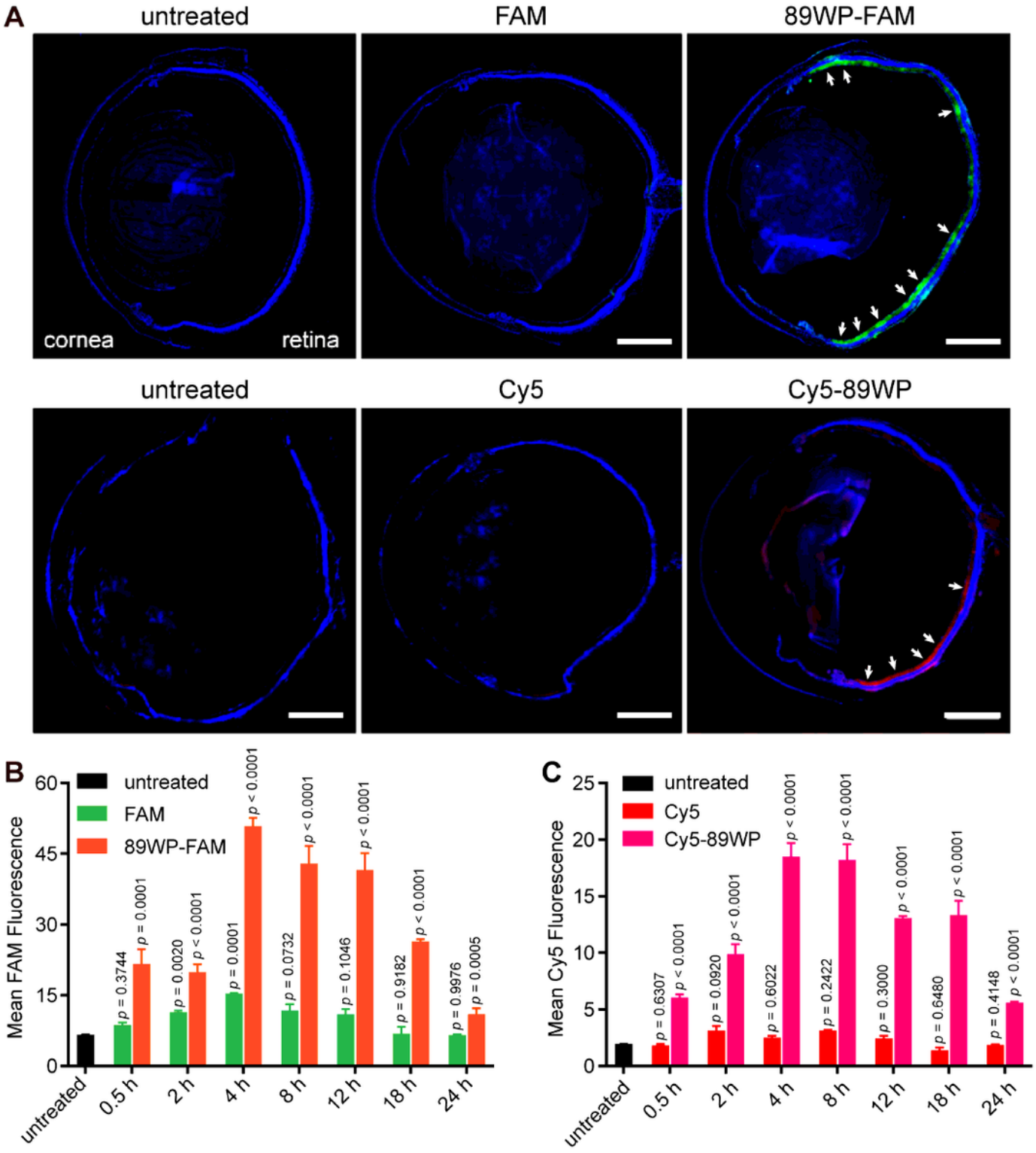

Figure 6

Distribution of topically instilled 89WP-FAM or Cy5-89WP in mice eyes. A, DAPI-stained frozen sections of the whole eyes from the treated mice. Eyes were harvested at 4 h after the instillation. Scale bar, 500 μm. B, C, Semi-quantitative analysis of time-dependent distribution of conjugates in DAPI-stained retina from treated mice. Eyes were harvested at 0.5 h, 2 h, 4 h, 8 h, 12 h, 18 h and 24 h after the instillation. Each retina (circled by the orange dash line in Fig. S10) was divided into five regions from top to bottom in the

sections, and the mean values of fluorescence intensity were calculated by ImageJ software. The statistical significance was analyzed by One-way ANOVA multiple comparisons corrected by Dunnett's test (n = 5). 89WP-FAM or Cy5-89WP was dissolved in 10 μL normal saline at a concentration of 30 μM and instilled into the conjunctiva sac of the mice.

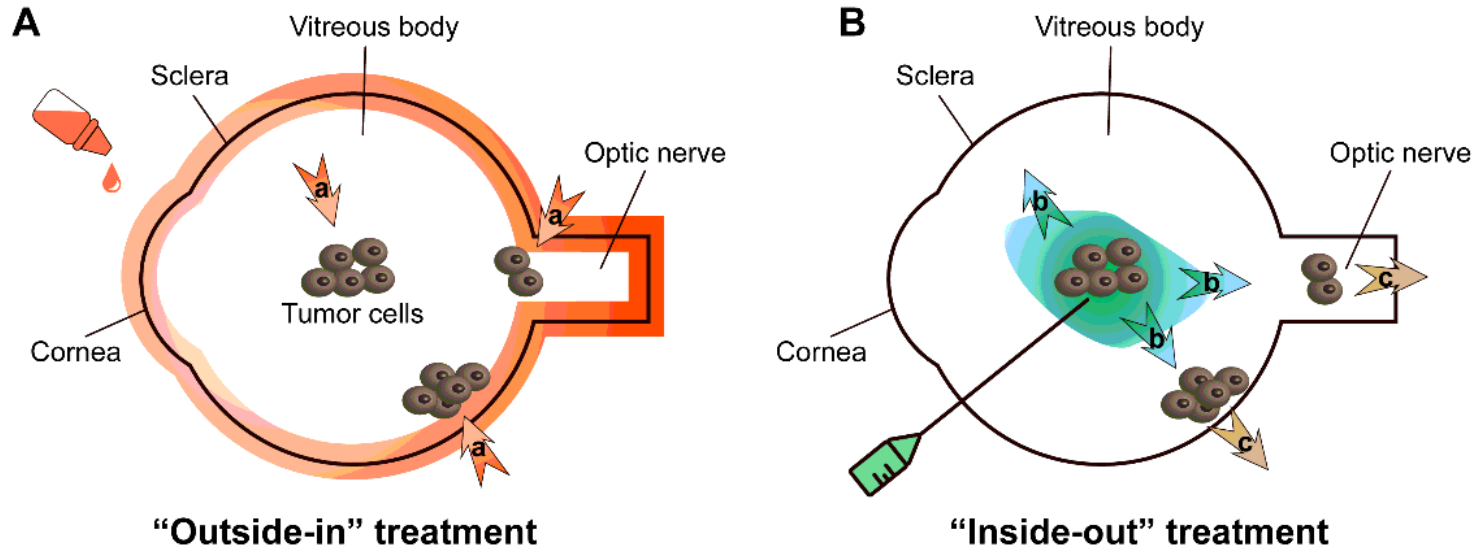

Figure 7

Anti-tumor mechanisms of melphalan via different administration routes. A, The topically instilled 89WP-Mel was absorbed in an "outside-in" manner. B, Intravitreally injected melphalan diffused in an "inside-out" manner. The labels were as following: a, intraocular diffusion directions of topically instilled 89WP-Mel; b, intraocular diffusion directions of intravitreally injected melphalan; c, intraocular tumor metastases directions, through optic nerve or the wall of eyeball.

Supplementary Files

This is a list of supplementary files associated with this preprint. Click to download.

- Supportinginformation20210805.docx
- RS1.pdf